Catal Lett (2016) 146:937–944
DOI 10.1007/s10562-016-1713-x

Silver–Alumina Catalysts for Low-Temperature Methanol Incineration

Magdalena Jabłońska[1] · Marek Nocuń[2] · Ewa Bidzińska[1]

Received: 3 February 2016 / Accepted: 4 February 2016 / Published online: 20 February 2016

Abstract The use of methanol as an alternative fuel for gasoline or diesel engines increases the unregulated CH_3OH emission. γ-Al_2O_3 modified with Cu, Mn, Ce, K, Ag, Cu–Mn, Cu–Ce, Cu–Ag or Cu–K (0.5, 1.0, 0.5:0.5, 1.0:1.0 wt% of metal) catalysed the process of methanol incineration. The highest activity reached samples containing 1.0 wt% of silver. Dispersed Ag^+ species on Al_2O_3 served as active species for selective oxidation of CH_3OH to CO_2 over both Ag/Al_2O_3 and $Cu–Ag/Al_2O_3$. Additionally, the XPS and EPR results revealed the AgO interface between the Ag_2O and CuO in the Cu–Ag system.

Graphical Abstract

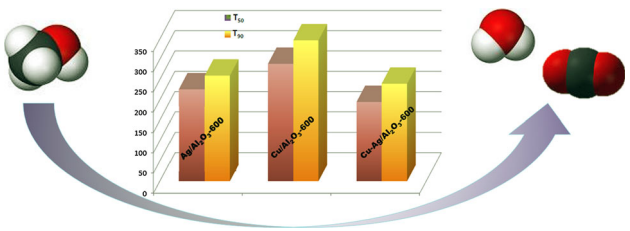

Keywords Alumina · Silver · Catalytic properties · Methanol incineration · VOCs

✉ Magdalena Jabłońska
Magdalena.Jablonskaw@gmail.com

[1] Faculty of Chemistry, Jagiellonian University, Ingardena 3, 30-060 Kraków, Poland

[2] Faculty of Material Science and Ceramics, AGH University of Science and Technology, Mickiewicza 30, 30-059 Kraków, Poland

1 Introduction

Volatile organic compounds (VOCs) are organic compounds with the boiling points lower than 260 °C at a standard atmospheric pressure of 101.325 kPa. VOCs are recognized as major contributors to air pollution because of their toxicity in living organisms, especially in humans and their involvement in the formation of photochemical smog [1]. The catalytic combustion is currently considered as the most promising method in order to reduce emissions of volatile organic compounds into the atmosphere. The catalysts of VOCs combustion can be divided into two main groups: (i) noble metal catalysts and (ii) transition metal oxides (e.g. [2, 3]). The most commonly used carrier for the active phases is γ-Al_2O_3 (e.g. [4]). Detailed information about mentioned catalytic systems were given in comprehensive reviews (e.g. [1, 5, 6] etc.). The catalysts containing platinum and palladium are the most widely implemented in practice due to their remarkable activity. E.g. among tested palladium supported on γ-Al_2O_3 (0.5–2.5 wt% of Pd), the catalyst with palladium content of 1.0 wt% revealed maximum methanol oxidation at 225 °C [3]. Silver-based catalysts have been less intensively studied for total combustion of VOCs. The studies of Cordi and Falconer [7] led to the conclusion that the Ag/Al_2O_3 (2.1 wt% of Ag), was very active for the complete oxidation of various VOCs. Based on the largest CO_2 peak (based on TPO analysis), it was suggested, that the relative oxidation activities followed the order:

formic acid > methanol > acetic acid > ethanol > acetaldehyde.

The silver supported on alumina was studied for oxidation of toluene (e.g. [8]) or acetone and pyridine

oxidation [9]. E.g. optimum loading for the complete oxidation of toluene reached 11.0 wt% for Ag/Al_2O_3. The addition of copper (1.0–5.0 wt%) provided complete toluene oxidation at 250–260 °C [9]. Additionally, HY and HZSM-5 zeolites doped with silver (2.5–3.9 wt%) were utilized for ethyl acetate with its total combustion around 350–400 °C (e.g. [10, 11]). Ag/HY (1.0 wt% of Ag) showed also activity for both toluene and methyl ethyl ketone with total oxidation below 350 °C [12]. Besides silver-based catalytic systems, a lot of studies report successful application of the Cu-containing catalysts for VOCs elimination (including methanol) (e.g. [2, 13]).

Methanol is mainly used in automobiles—an additive or an alternative fuel for gasoline engines—due to its ability to produce power with lower emission of air pollutants (e.g. [14]). However, a large amount of methanol may be emitted as a result of its incomplete combustion [15]. The solution for its escape to the atmosphere could be catalytic oxidation of unburned methanol from exhaust gases. Depending on methanol blended fuels, applications temperature of exhaust gases may vary in the range of 300–450 °C for spark ignition engines [16] or below 200–300 °C for diesel engines (e.g. [14]).

In the present paper, we report results of the screening study of alumina-based catalysts in the range from 150 to 450 °C. Moreover, we included detailed physicochemical characterization, such as: structural (XRD, EPR) and textural (BET) analysis; redox properties (H_2-TPR) and chemical surface composition (XPS). Our attention focused on the characterization of the active species of these catalytic systems.

2 Experimental

2.1 Catalysts preparation

γ-Al_2O_3 (Merck) was doped with Cu, Mn, Ce, K, Ag, by the incipient wetness impregnation method using aqueous solutions of the following metal nitrates: $Cu(NO_3)_2{\cdot}3H_2O$ (Merck), $Mn(NO_3)_2{\cdot}4H_2O$ (Lach-Ner), $Ce(NO_3)_3{\cdot}6H_2O$ (POCH), KNO_3 (CHEMPUR), $AgNO_3$ (POCH). The sequence of metal deposition in case of bimetallic systems were as follows: Cu–Mn, Cu–Ce, Cu–Ag or Cu–K. Based on preliminary studies over alumina modified with palladium [3], samples were modified with two concentrations of metals, such as 0.5 or 1.0 wt%. E.g. samples denoted as (1.0 wt%) $Cu–Mn/Al_2O_3$ contained 1.0 wt% of each of the deposited metal. All prepared samples were dried and subsequently calcined in static air at 600 °C for 12 h. For catalytic experiments, a sieve fraction of particles with size of 0.160–0.315 mm was used.

2.2 Catalytic tests

All prepared materials were tested as catalysts in total methanol oxidation. The catalytic experiments were performed under atmospheric pressure in a fixed-bed flow microreactor system. The reactant concentration were continuously measured using a quadruple mass spectrometer RGA 200 (PREVAC) connected directly to the reactor outlet. Prior to the catalytic test, each sample of the catalyst (100 mg) was outgassed in a flow of synthetic air at 500 °C for 30 min. The isothermal saturator placed in an ice-water bath and with a constant flow of synthetic air was used for supplying of methanol into the reaction mixture. The composition of gas mixture at the reactor inlet was $[CH_3OH] = 4.0$ vol%, $[O_2] = 19.0$ vol% and $[N_2] = 77.0$ vol%. Total flow rate of the reaction mixture was 20 cm^3/min.

2.3 Catalysts characterization

The X-ray diffraction (XRD) patterns of the samples were recorded with a D2 Phaser diffractometer (Bruker) using Cu Kα radiation ($\lambda = 1.54060$ Å, 30 kV, 10 mA).

The specific surface area (S_{BET}) of the samples was determined by low-temperature (−196 °C) N_2 sorption using Quantasorb Junior sorptometer (Ankersmit). Prior to nitrogen adsorption the samples were outgassed at 250 °C for 2 h in a flow of N_2.

The temperature-programmed reduction (H_2-TPR) patterns of samples (30 mg) were performed using using a Quantachrome ChemBET Pulsar TPR/TPD instrument. H_2-TPR runs were carried out starting from room temperature to 800 °C, with a linear heating rate of 10 °C/min and in a flow (6 cm^3/min) of 5 vol% H_2 diluted in Ar. Water vapour was removed from effluent gas by the means of a cold trap placed in an ice-water bath. The H_2 consumption was detected and recorded by TCD.

X-ray photoelectron spectra (XPS) were measured on a VSW spectrometer equipped with a hemispherical analyser. The photoelectron spectra were measured using a magnesium MgKα source (E = 1253.6 eV). The base pressure in the analysis chamber during the measurements was 3×10^{-6} Pa and the spectra were calibrated on a main carbon C 1s peak at 284.6 eV. The composition and chemical surrounding of the sample surface were investigated based on the areas and binding energies of Ag 3d, Cu 2p, Al 2p, C 1s and O 1s photoelectron peaks. Mathematical analyses of the XPS spectra were carried out using the XPSpeak 4.1 computer software (RWM. Kwok, The Chinese University of Hong Kong).

The electron paramagnetic resonance (EPR) spectra were recorded at room temperature using an ELEXSYS E-500 spectrometer (Bruker) operating at the 100 kHz field

modulation. Prior to EPR measurements the samples were outgassed under high vacuum. In order to determine the integral intensity of the EPR spectra, double integrals of spectra were calculated.

3 Results and discussion

3.1 Catalytic activity

Alumina modified with different metals was tested in the process of methanol incineration. Figure 1 presents obtained results, while Table 1 summarizes T_{50} and T_{90} for the studied catalysts. T_{50} refers to the temperature needed to reach 50 % methanol conversion, and it is widely use to compare catalytic activity in the same reaction conditions, while T_{90} is the temperature needed to obtain 90 % methanol conversion. The obtained results showed full methanol conversion over all tested catalysts in the temperature range of 125–450 °C. The exception was pure oxide support, for which 94 % conversion of methanol was achieved at 450 °C (Fig. 1a). In the case of a catalyst containing 1.0 wt% of copper, complete conversion of the methanol was achieved at 400 °C. The addition of the promoter, such as 0.5 and 1.0 wt% of potassium, resulted in both cases in a slight increase in catalytic activity with respect to Cu/Al_2O_3 (Fig. 1b). Activating effect of potassium on copper catalysts is consistent with literature data (e.g. [13]).

The low activity of catalyst containing only manganese was obtained especially in the low temperature range. However, complete conversion of methanol over such catalytic system was reached at 375 °C. In the scientific literature, manganese-containing materials are highly active catalysts of VOCs combustion, such as toluene, ethanol and butanol (e.g. [17, 18]). The addition of manganese (0.5 or 1.0 wt%) to a sample containing copper increased its catalytic activity, however only above 300 °C (Fig. 1b). The total conversion of methanol over (1.0 wt%)Mn–(1.0 wt%)Cu/Al_2O_3 was achieved at 325 °C—at temperature lower of about 75 °C compared to that obtained for (1.0 wt%)Cu/Al_2O_3. Such results are in agreement with literature data, which showed that doping with manganese improved catalytic activity of the Cu-containing samples (e.g. [18]).

Increasing cerium content in the catalyst resulted in an increase in activity, but the value for methanol conversion was still lower than that of the sample containing the same amount of copper in the sample (Fig. 1a). The bimetallic (Cu–Ce) catalysts were more active compared to Cu/Al_2O_3 only below 350 °C (Fig. 1b). On the other side, in the scientific literature the Cu–Ce systems are widely discussed as potential commercial catalysts for VOC

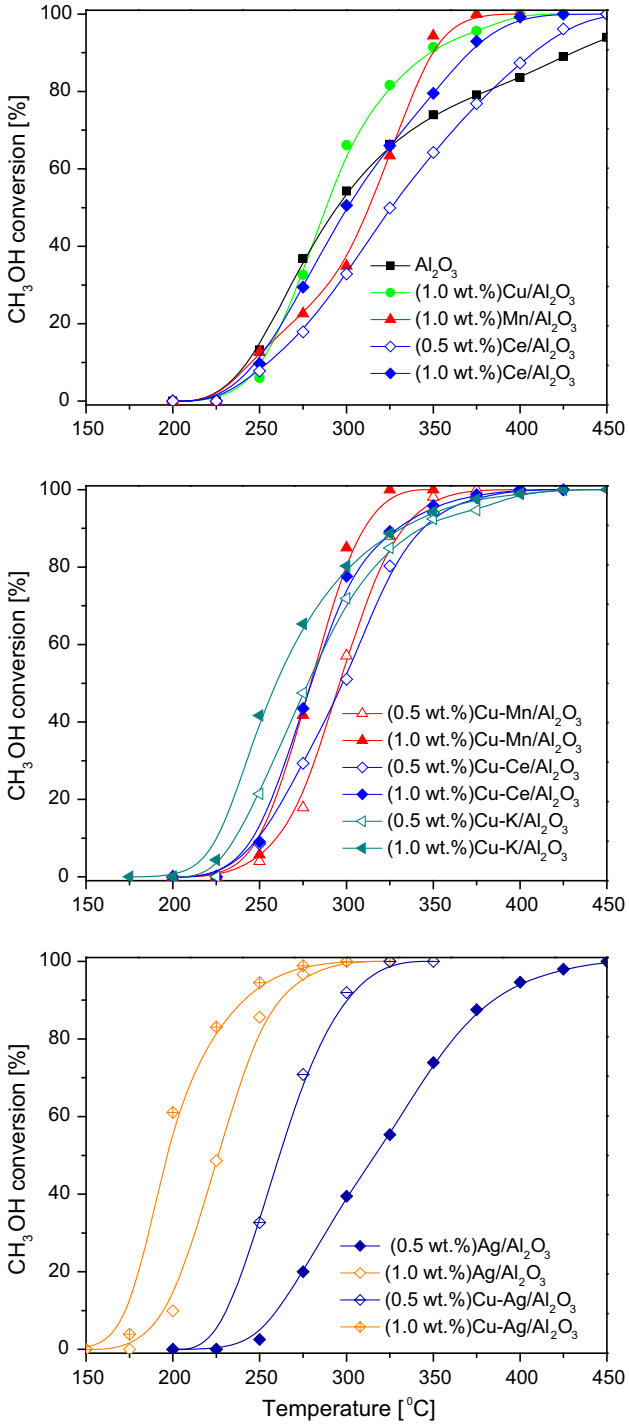

Fig. 1 Total incineration of methanol performed in the presence of commercial alumina and alumina-based catalytic materials. Reaction conditions: mass of catalyst = 100 mg, $[CH_3OH]$ = 4.0 vol%, $[O_2]$ = 19.0 vol% and $[N_2]$ = 77.0 vol%, total flow rate = 20 cm^3/min, linear heating of 10 °C/min

combustion (e.g. [19]). Such discrepancies could be explained by different preparation methods, used supports as well as reaction conditions. An increase of catalytic activity with increasing metal content in the samples was

Table 1 T_{50} and T_{90} temperatures of methanol incineration over catalysts and specific surface areas (S_{BET}) of the catalytic materials

Sample codes	T_{50} (°C)	T_{90} (°C)	S^{BET} (m^2/g)
Al_2O_3	295	431	135
(1 wt%)Cu/Al_2O_3	289	347	98
(1 wt%)Mn/Al_2O_3	314	347	99
(0.5 wt%)Ce/Al_2O_3	326	407	92
(1 wt%)Ce/Al_2O_3	299	368	91
(0.5 wt%)Ag/Al_2O_3	317	386	91
(1 wt%)Ag/Al_2O_3	226	260	89
(0.5 wt%)Cu–Mn/Al_2O_3	296	330	100
(1 wt%)Cu–Mn/Al_2O_3	280	308	82
(0.5 wt%)Cu–Ce/Al_2O_3	299	346	90
(1 wt%)Cu–Ce/Al_2O_3	280	330	86
(0.5 wt%)Cu–K/Al_2O_3	278	343	87
(1 wt%)Cu–K/Al_2O_3	259	333	85
(0.5 wt%)Cu–Ag/Al_2O_3	261	297	93
(1 wt%)Cu–Ag/Al_2O_3	195	240	88

also observed for silver-based catalysts (Fig. 1c). The increase in the silver loading from 0.5 to 1.0 wt% greatly improved catalytic activity in the methanol incineration, and consequently its complete conversion over (1.0 wt%)Ag/Al_2O_3 occurred at 300 °C. Furthermore, the bimetallic Cu–Ag systems showed a higher value for methanol conversion (especially below 275 °C) compared to Ag-doped samples. However, the full conversion of methanol for all samples containing 1.0 wt% of silver was reached at 300 °C. Analyzing the summarized results for the studied catalysts (Table 1), it could be concluded that among all utilized materials, the most active catalysts was the one containing 1.0 wt% of silver—with T_{90} of 260 and 240 for Ag/Al_2O_3 and Cu–Ag/Al_2O_3, respectively. CO_2 and water vapour were the only detected reaction products over both catalysts using QMS analysis.

3.2 Physicochemical properties of the catalysts

Figure 2 presents the powder XRD diffraction pattern obtained for the commercial alumina. Characteristic XRD diffraction peaks corresponding to the reflections of γ-Al_2O_3 were located at 19.9°, 32.6°, 37.5°, 39.6°, 45.9°, 61.1° and 67.0° [20]. No changes in the structure of oxide support appeared after impregnation with metals (results not shown).

Table 1 shows the specific surface areas (S_{BET}) of alumina and its modifications with metals. Deposition of metals on the oxide support surface resulted in a decrease of specific surface areas (82–100 m^2/g) due to surface covering by the low surface area clusters of active components.

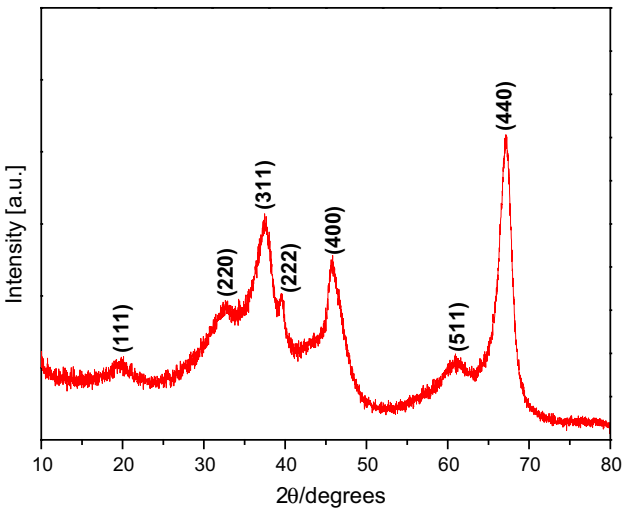

Fig. 2 XRD pattern of commercial γ-Al_2O_3

Figure 3 presents the H_2-TPR profiles of copper and/or silver modified alumina. No reduction peaks appeared in the profiles recorded for pure γ-Al_2O_3. Two peaks centered around 110 and 385 °C appeared for Ag/Al_2O_3; thus indicating two different silver oxide species. According to literature reports (e.g. [9, 21]), the first peak was ascribed to the highly dispersed Ag_2O, while the second one to the more aggregated Ag_2O. The reduction profile of pure Ag_2O consisted on a single peak at 250 °C, as it was reported earlier by Luo et al. [9]. They also investigated redox behaviour of Ag/Al_2O_3 and claimed three kinds of Ag_2O of different chemical environments in catalysts—the crystal Ag_2O phase together with dispersed Ag_2O phases (I,II), while the reduction of the former was reported to be easier than of the latter. However, in this studies, any silver oxide phases were identified in Ag/Al_2O_3. Therefore, the second peak was ascribed to the reduction of Ag_2O clusters on the γ-Al_2O_3, according to indications of Musi et al. [21].

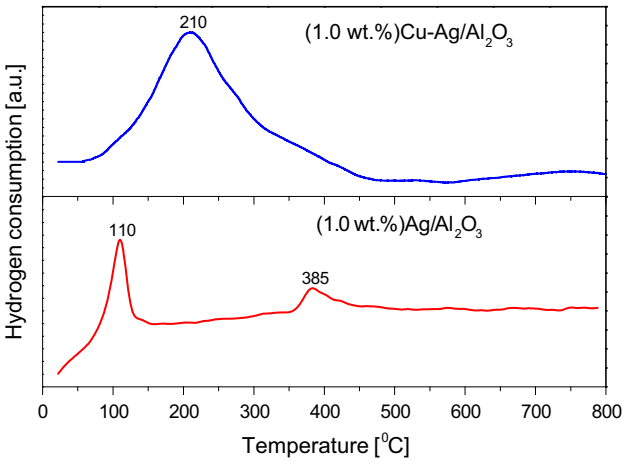

Fig. 3 TPR patterns of Ag/Al_2O_3 and Cu–Ag/Al_2O_3

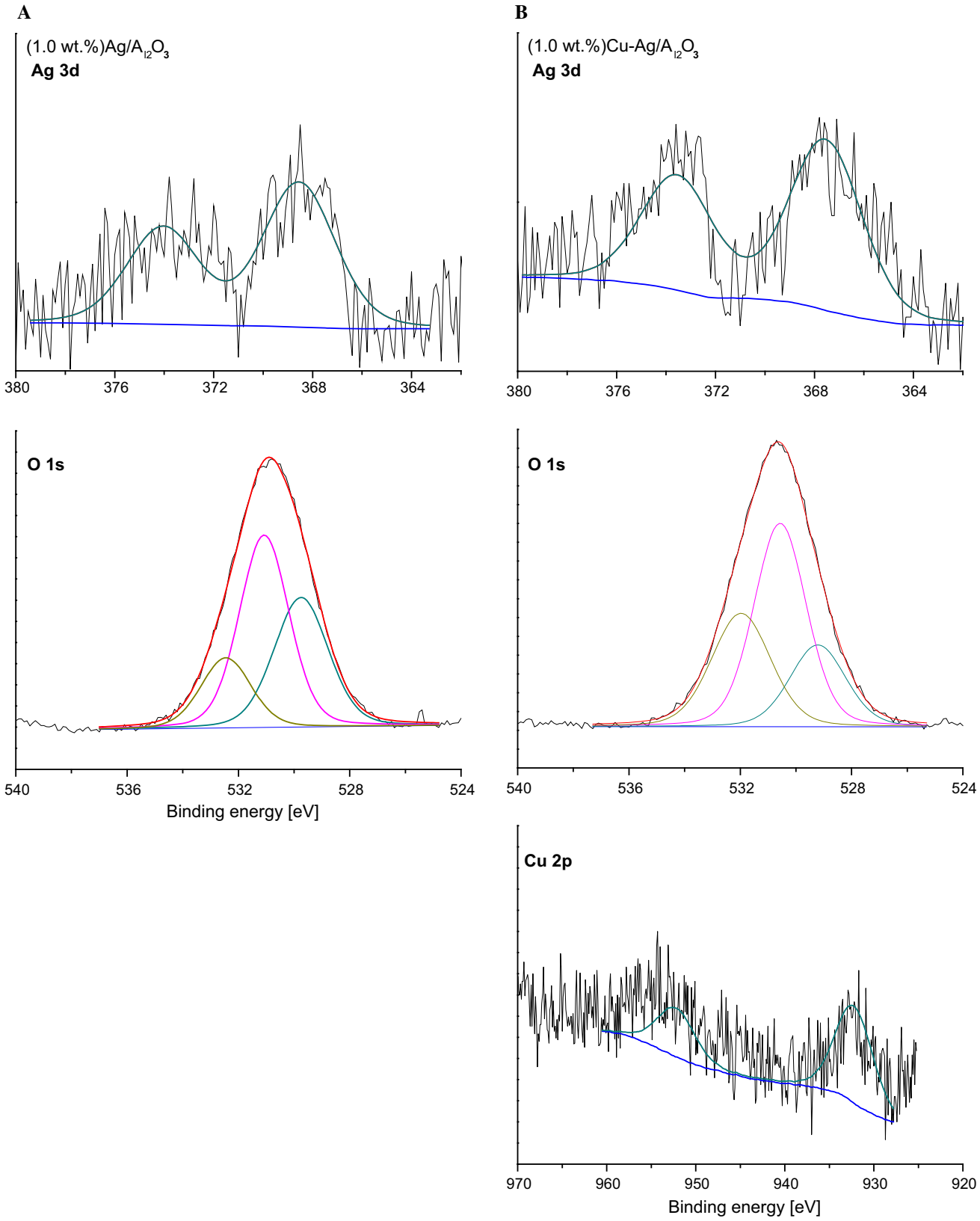

Fig. 4 XP spectra in the range of binding energies for Ag/Al_2O_3 (**a**) and $Cu–Ag/Al_2O_3$ (**b**)

The TPR pattern of (1.0 wt%)Cu/Al_2O_3 with main peak centred at about 304 °C was presented in our earlier studies [22]. Additionally, deposition of silver decreased the reduction temperature of the highly dispersed copper oxide species to 210 °C. The bimetallic species can form either alloys or segregated core–shell structures (e.g. [23, 24]), which could be reduced at temperatures lower than pure copper oxide species. On the other side, Cu-Ag alloys were reported to be thermodynamically unstable (e.g. [25]). The transmission electron microscopy (TEM) studies over Cu–Ag/Al_2O_3 (2.5, 7.5 wt% of Cu, 2.5, 7.5 wt% of Ag) revealed intimate contact between copper and silver [25]. Consequently, the authors suggested that catalysts structure consists of a highly dispersed copper oxide (monolayer) on alumina upon which silver particles (of a very wide particle-size distribution) were situated. The proposed model seems to be valid also in case of our studies.

More information of the silver and copper state on the surface of alumina was obtained from XPS and EPR studies. Figure 4 and Table 2 summarize the X-ray photoelectron spectroscopy (XPS) results of (1.0 wt%)Ag/Al_2O_3 and (1.0 wt%)Cu–Ag/Al_2O_3. The most intense peak of Ag 3d occurred at about 368.8 and 368.1 eV for the Ag/Al_2O_3 and Cu–Ag/Al_2O_3, respectively. According to literature data, XPS peaks at 368.1–367.9 and 374.1–373.9 eV were ascribed to metallic Ag $3d_{5/2}$ and Ag $3d_{3/2}$. Additionally, the Ag $3d_{5/2}$ BE values in the range 367.7–367.6 eV are characteristic of Ag_2O, while AgO range from 367.4 to 367.2 eV [26]. However, many factors could influence the position of XPS peaks, including nature of the support and surrounding oxide species. Therefore, the XP peaks spectra of both samples were attributed to Ag_2O species. Interestingly, according to the scientific indications the bonding energy of Ag $3d_{5/2}$ for the bimetallic catalyst samples, i.e. Cu–Ag, have been reported to have positive peak shift compared to pure Ag/Al_2O_3 (e.g. [24, 27]). On the other side, these results were obtained for materials after reduction with hydrogen. In our case, the binding energy for the Cu–Ag/Al_2O_3 sample had negative peak shift (368.8 eV → 368.1 eV). Moreover, Ag 3d peak became slightly broader with a full width at half-maximum (FWHM) from 3.4 to 3.5 eV. Thus, such effect was attributed to the possible generation of Ag^{2+} species as a result of strong interactions between silver and copper oxide species in Cu–Ag/Al_2O_3. These findings could be supported by XPS studies of Prieto et al. [23] over silver-nickel nanoparticles (NPs) prepared by seed-mediated growth. The BE of Ag 3d for Ag–Ni NPs shifted towards lower values signifying the existence of oxidized silver.

Taking into account copper in the Cu–Ag/Al_2O_3 sample, the most intensive peak of Cu 2p occurred at about 932.5 eV and was attributed to the Cu^{2+}. These results were fully consistent with data presented by Gang et al. [25].

The results gained in both H_2-TPR and XPS measurements fully correspond with the EPR analysis. Figure 5a shows, that the EPR spectrum of Ag/Al_2O_3 sample revealed a very low intensity. Several authors reported that

Table 2 XPS results of Ag/Al_2O_3 and Cu–Ag/Al_2O_3

Sample code	Peak	Position[a] (eV)	FWHM[b]
(1.0 wt%)Ag/Al_2O_3	Ag 3d	368.8	3.4
	O 1s	529.8	2.3
		531.1	2.1
		532.5	2.1
(1.0 wt%)Cu–Ag/Al_2O_3	Ag 3d	368.1	3.5
	O 1s	529.3	2.4
		530.7	2.2
		532.1	2.5
	Cu 2p	932.5	5.0

[a] Position of binding energy, [b] Full width at half-maximum

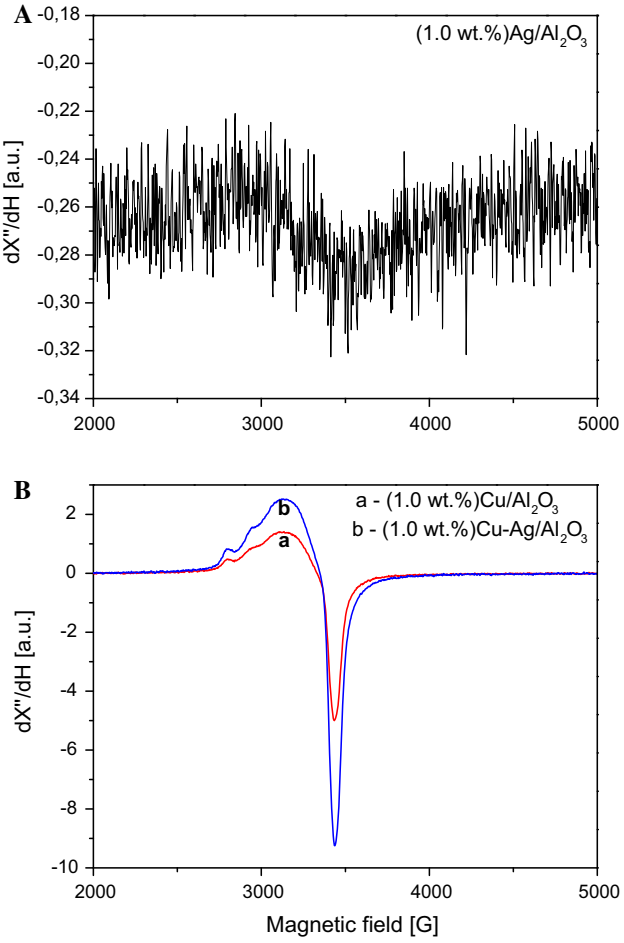

Fig. 5 EPR spectra of Ag/Al_2O_3 (**a**), Cu/Al_2O_3 and Cu–Ag/Al_2O_3 (**b**)

Ag^{2+} ions can provide signal at $g_{iso} \approx 2.20–2.30$ [28]. Thus, it can be concluded that only traces of Ag^{2+} were present in this sample. Since Ag^{+} ions are diamagnetic, therefore, it could be stated that the silver was present in the sample mainly in the form of Ag_2O.

Spectra of Cu/Al_2O_3 and $Cu–Ag/Al_2O_3$ (Fig. 5b) were typical for Cu^{2+} present in a magnetic environment having axial symmetry ($g_{\perp} = 2.04$ and $g_{\parallel} = 2.21$) [29]. Thus, the obtained results indicated the presence of CuO in both samples. The weakly visible hyperfine structure originating in magnetic momenta of ^{63}Cu and ^{65}Cu nuclei ($I = 3/2$) suggested the formation of small copper(II) oxide clusters. Comparing the intensities of spectra for samples containing the same copper loading (1.0 wt%), it should be noted, that in the case of $Cu–Ag/Al_2O_3$, the integral intensity of the spectrum was about 60 % higher than the intensity of Cu/Al_2O_3. Therefore, silver was possibly in the form of magnetically active Ag^{2+} or Ag^{0}. The high calcination temperature of 600 °C (12 h, static air), the same charges of Ag^{2+} compared to Cu^{2+} ions and their similar g_{iso}, suggested that the increase in intensity originates from the presence of Ag^{2+}. Following results were consistent with XPS interpretation in which comparing Cu/Al_2O_3 and $Cu–Ag/Al_2O_3$ samples, it was found that in the second sample there is more Ag^{2+}. The results did not resolve the speciation of silver ions. Any evidence of metallic form of silver was found. Nevertheless, further detailed studies—and with different combinations of Cu–Ag—proceeds to justify such findings.

4 Conclusions

Methanol as renewable and alternative energy source for the gasoline or diesel engine gain importance. Unregulated methanol emissions are one of the most serious concern regarding the use of low-content methanol applications. Therefore, suitable catalytic systems are highly required to meet future regulations.

In this study, we carried out a screening research of the activity of a series of catalysts—γ-Al_2O_3 modified Cu, Mn, Ce, K, Ag, Cu–Mn, Cu–Ce, Cu–Ag, Cu–K—for the total methanol oxidation. The silver-based catalysts were very active for methanol incineration. An order of activity based on T_{90} over bimetallic catalytic systems with 1.0 wt% of metals were found as follows: Ag–Cu > Mn–Cu > Ce–Cu > K–Cu. The Ag^{+} species dispersed on alumina were responsible for high catalytic activity. Additionally, the XPS and EPR results confirmed the presence of Ag^{2+} at the interface between the Ag_2O and CuO.

Further studies are underway on activity and stability of Cu–Ag system at lower methanol concentration as well as under real conditions of exhaust gases.

Acknowledgments Part of the research was done with equipment purchased in the frame of the European Regional Development Fund (Polish Innovation Economy Operational Program – Contract No. POIG.02.01.00-12-023/08).

References

1. Li WB, Wang JX, Gong H (2009) Catal Today 148:81
2. Jabłońska M, Chmielarz L, Węgrzyn A, Góra-Marek K, Piwowarska Z, Witkowski S, Bidzińska E, Kuśtrowski P, Wach A, Majda D (2015) Appl Clay Sci 114:273
3. Jabłońska M, Król A, Kukulska-Zając E, Tarach K, Girman V, Chmielarz L, Góra-Marek K (2015) Appl Catal B 166–167:353
4. Müller H, Deller K, Despeyroux B, Peldszus E, Kammerhofer P, Kuhn W, Spielmannleitner R, Stronger M (1993) Catal Today 17:383
5. Rusu AO, Dumitriu E (2003) Environ Eng Manag J 4:273
6. Huang H, Xu Y, Feng Q, Leung DY (2015) Catal Sci Technol 5:2649
7. Cordi EM, Falconer JL (1997) Appl Catal A 151:179
8. Kim SCh, Ryu JY (2011) Environ Technol 32:561
9. Luo MF, Yuan XX, Zheng XM (1998) Appl Catal A 175:121
10. Jodaei A, Salari D, Niaei A, Khatamian M, Çaylak N (2011) Environ Technol 32:395
11. Wong ChT, Abdullah AZ, Bhatia S (2008) J Hazard Mater 157:480s
12. Baek SW, Kim JR, Ihm SK (2004) Catal Today 93–95:575
13. Chmielarz L, Piwowarska Z, Rutkowska M, Wojciechowska M, Dudek B, Witkowski S, Michalik M (2012) Catal Commun 17:118
14. Yusaf T, Hamawand I, Baker P, Najafi D (2013) Int J Automot Mech Eng 8:1385
15. Zhang F, Wang JH, Tian DL, Wang JX, Shuai SJ, SAE Technical Paper 2013-01-1345
16. Devi EN, Bhatti SK, Priyadarsini ChI, MuraliKrisha MVS (2013) Int J Eng Res Appl 1351
17. Zimowska M, Michalik-Zym A, Janik R, Machej T, Gurgul J, Socha RP, Podobiński J, Serwicka EM (2007) Catal Today 119:321
18. Aguilera DA, Perez A, Molina R, Moreno S (2011) Appl Catal B 104:144
19. Dziembaj R, Molenda M, Zaitz MM, Chmielarz L, Furczoń K (2013) Solid State Ion 251:18
20. Wan H, Li D, Dai Y, Hu Y, Liu B, Dong L (2010) J Mol Catal A 332:32
21. Musi A, Massiani P, Brouri D, Trichard JM, Da Costa P (2009) Catal Lett 128:25
22. Jabłońska M (2015) Chem Papers 69:1141
23. Prieto P, Nistor V, Nouneh K, Oyama M, Abd-Lefdil M, Díaz R (2012) Appl Surf Sci 258:8807
24. Czaplińska J, Sobczak I, Ziółek M (2014) J Phys Chem C 118:12796
25. Gang L, Anderson BG, Van Grondelle J, van Santen RA, van Gennip WJH, Niemantsverdriet JW, Kooyman PJ, Knoester A, Brongersma HH (2002) J Catal 206:60

26. Huang Y, Ariga H, Zheng X, Duan X, Takakusagi S, Asakura K, Yuan Y (2013) J Catal 307:74
27. Wang HK, Yi ChY, Tian L, Wang WJ, Fang J, Zhao JH, Shen WG (2012) J Nanomater 2012:4
28. Wang YP, Yeh CT (1991) J Chem Soc, Faraday Trans 87:345
29. Aboukaïs A, Bennani A, Aissi CF, Wrobel G, Guelton M (1992) J Chem Soc, Faraday Trans 88:615